Advances in Science and Technology Research Journal

Advances in Science and Technology Research Journal 2023, 17(3), 309–319
https://doi.org/10.12913/22998624/167451
ISSN 2299-8624, License CC-BY 4.0

Received: 2023.04.25
Accepted: 2023.05.19
Published: 2023.06.06

Validation of Extension-Bending and Extension-Twisting Coupled Laminates in Elastic Element

Katarzyna Falkowicz[1]

[1] Faculty of Mechanical Engineering, Department of Machine Design and Mechatronics, Lublin University of Technology, Nadbystrzycka 36, 20-618 Lublin, Poland
e-mail: k.falkowicz@pollub.pl

ABSTRACT

The article deals with the design of the stacking sequence of layers in composite plate element in order to create the desired behaviour in the postcritical range. Tested plates were made of carbon fiber reinforced polymer (CFRP) laminate with different layer arrangement. As the type of load, the axial compression was assumed. The configurations have been choosen specifically to investigate the influence of *Extension-Twisting* and *Extension-Bending* coupled designs under axial load. To analyse the influence of layer arrangement on the posbuckling behaviour the parametric study was performed. Matlab software and a script developed by the author were used to calculate the components of ABD matrix. Additionally, the experimental validation was carried out together with numerical analysis.

Keywords: extension-twisting coupling, extension-bending coupling, Finite Element Method, coupled laminates, asymmetrical configuration, post-buckling behavior, experimental tests

INTRODUCTION

This article is one of a series addressing to unifed approach to use the asymmetric configurations of composite, having a mechanical couplings in order to create the desired behaviour of element. In this case to obtain the elastic element. It is worth emphasizing here that thin-walled structures made of laminates provide great flexibility in their design behaviour.

Among the most popular we can mention designing a sequence of layers for predictability deflection of structures subjected to operational load.

Many scientist papers described the influence of the symmetrical laminate layer arrangement on the behavior of thin-walled structures. For example Debski et al. [1,2] carried out the compression tests of CFRP (*Carbon Fiber Reinforced Polymer*) thin-walled structures with different kind of cross-section and with different layer configuration. Kubiak et al. [3] tested the influence of different layer arrangements (symmetrical and nonsymmetrical) of GFRP (*Glass Fiber Reinforced Polymer*) polymer on the distortional postbucklin behavior of open section beams. Banat and Mania [4] presented an analysis of the symmetric configurations of FML until failure. Wysmulski tested sensitivity of compressed composite channel columns with different configurations to eccentric loading [5,6]with each layup having eight plies symmetric to the midplane. The columns were subjected to compressive loads, including an eccentric compressive load applied relative to the center of gravity of their cross-section. Simple support boundary conditions were applied to the ends of the columns. The scope of the study included analyzing the effect of load eccentricity on the buckling mode, bifurcation load (idealized structure.

Recently, more attention has been focused on composites in an asymmetrical configuration. This kind of laminates with complex mechanical couplings can find application not only the aerospace sector, with which they have been

traditionally associated. They offer great potential as for example an enabling technology in very large offshore wind turbine blades. Ch. York in his recent research [7] has shown that is some unexplored laminate design area containing different kind of mechanical coupling, which includes all interactions between extension, bending, shearing and twisting. Furthermore, he analyzed laminate stacking sequences which are immune to thermal warping distortions [8]. York and Lee [9] performed experimental validation of recently identified laminates possessing *Hygro-Thermally Curvature Stable* or HTCS properties [10]. Teter et al. [11] analyzed the effect of individual elements of the B submatrix on the load-carrying capacity of a hybrid column. Some examples of analytical work on the nonlinear analysis of plates, with asymmetric configurations, has been assembled in work [12] and [13]. A detailed description of stiffness matrix couplings for asymmetric laminates are presented in works Altenbach [14] and Samborski [15,16].

To assess the performance benefits, such as twist angle, interactions between Extension, Shearing, Bending and Twisting couplings of nonsymetric composites, the investigations of those structure are necessairy. What is more, suitable ply design can not only endow laminates with special coupling effect [17,18], but also can improve mechanical properties of laminates [19]. The analyses in this area may help to raise interest in the potential for exploiting mechanically coupled materials, particularly from a manufacturing perspective. Applications of the unique couplings inherent in asymmetric laminates can provide design advantages.

This study concerns thin-walled composite plate element, made of fibrous composite materials with different sequences of laminate layers, which includes all possible interactions between extension, shearing, bending and twisting. These complex mechanical couplings are not present in conventional materials, such as metals, and therefore, represent an important and significant enabling technology. The scope of the research includes the problems of nonlinear stability and failure of laminate coupled profiles subjected to uniform compression. The novelty of this research is to perform a parametric study with different nonsymmetrical layer arrangements with selected couplings, in order to check their influence on post-buckling behavior. Special attention has been paid to validation the effect of extension-bending and extension-twisting coupling.

EXPERIMENTAL TESTS

Research subject and laminate material properties

The samples for experimental tests were made of CFRP pre-preg manufactured using a standard autoclave technique. The samples had three layers arrangements in asymmetric configurations and with three considered fibre alngles (30°, ±45°, 60°). Additionally, the layer arrangement of plate core was also considered in the analytical calculations (N4). The laminate configurations were characterized by selected mechanical couplings thanks to them the considered plate element can work as elastic element (Tab. 1). The selection was based on the works of Ch. York [7,8]. To get the flexural-torsional buckling mode as the natural the lowest mode of buckling extension–twisting (E-T) and extension-bending (E-B) coupled laminate class has been chosen for consideration. This procedure were more described in previous articles [13,20,21]. The thickness of each single layer was constant – 0.105 mm. The overall dimensions of considered plate with the layer arrangement sequence are presented in Figure 1. The plate element were weakned by central rectangular cut-out with rounded radius. The radius was constant and in considered case one type of cut-out had been choosen (b×a = 40×100) [22].

The material properties of CFRP laminate used for samples have been determined in experimental

Table 1. The laminate configurations under consideration

Case ID	Layers No.	Layer configuration	Laminate type [23]	Considered Θ [°]
N1	18	$[0_3/\Theta/-\Theta/0/-\Theta/\Theta/-\Theta/\Theta/-\Theta/\Theta/90/\Theta/-\Theta/90_3]_T$	$A_SB_{lt}D_S$	30, 45, 60
N2	14	$[\Theta/-\Theta/0/\Theta/-\Theta/0/\Theta/-\Theta/\Theta/-\Theta/0/\Theta/-\Theta/0]_T$	$A_SB_FD_F$	30, 45, 60
N3	12	$[\Theta/-\Theta/-\Theta/\Theta/0/\Theta/-\Theta/\Theta/-\Theta/-\Theta/\Theta/0]_T$	$A_SB_FD_F$	30, 45, 60
N4 (core)	2	$[\Theta/-\Theta]_T$	$A_SB_tD_S$	30, 45, 60

Note: Θ – fibre angle, N1, N2, N3 – symbols of configurations.

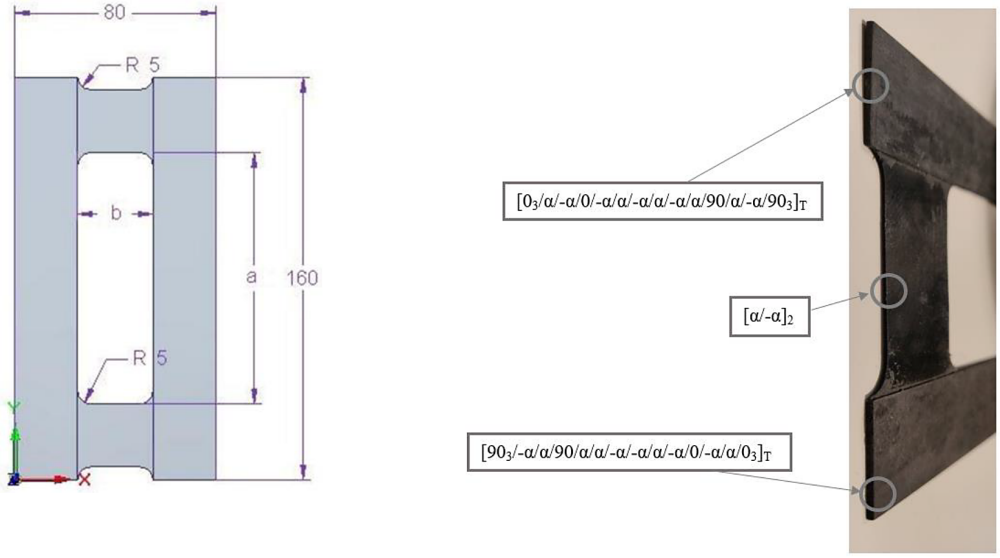

(a) (b)

Fig. 1. (a) The considered composite plate dimensions with (b) layer arrangement

Table 2. The material properties of the considered composite material

Young's modulus [MPa]		Shear modulus [MPa]	Poisson's ratio	Tensile strength [MPa]		Shear strength [MPa]	Compression strength [MPa]	
E_1 (0°)	E_2 (90°)	$G_{1,2}$	V_{12}	F_{TU1} (0°)	F_{TU2} (90°)	F_{SU} (45°)	F_{CU1} (0°)	F_{CU2} (90°)
143530	5826	3845	0,36	2221	49	83,5	641	114

tests according to ISO standards, which has been well described in paper [24]. The obtained material properties are presented in Table 2.

Axial compression tests

To validate the developed numerical models and to validate E-T and E-B couplings influence on plate behaviour, as well as to choose the most interesting cases for leading the parametric study, the experimental axial compression tests have been performed.

The experimental tests were performed on an Instron universal testing machine modernized by Zwick-Roel and equipped with specially designed grips (Fig. 2). The experimental tests were performed in room temperature at a constant velocity of the cross-bar equal 2 mm/min. During the tests, force loading, plate displacement and plate deflection in the perpendicular direction to the vertical stripes of the plate in the middle of the height of the stripe was measured. The values of the force loading the system and displacements at the load application points were obtained directly from the machine sensors. In addition, the DIC (*Digital Image Correlation*) technique (Aramis system produced by GOM company) was used to determine the deflection of the plate in the entire range of loads. What is more, the twist/rotation value was determined using the measurment of displacements of two points (dZ) located at the same height of the strip (see Fig. 2b,d). Based on the difference in deflections, we are able to estimate the level of twisting/rotation of the plate strips. The entire test stand presented in Figure 2. More informations about experimental tests are described in previous articles [21,25].

NUMERICAL MODEL

The numerical model has been developed in the commercial Abaqus software using the finite element method, which is now very widely used [26–30]. The tested plate elements were subjected to axial compression. The material properties of each layer of CFRP are the same as determined by experimental studies (Table 2). The FEM model, like geometry, the way of loading, boundary conditions were adopted as close as possible to those in the experimental test stand (Fig. 2).

All plate elements corresponded to the tested specimens and were modelled using

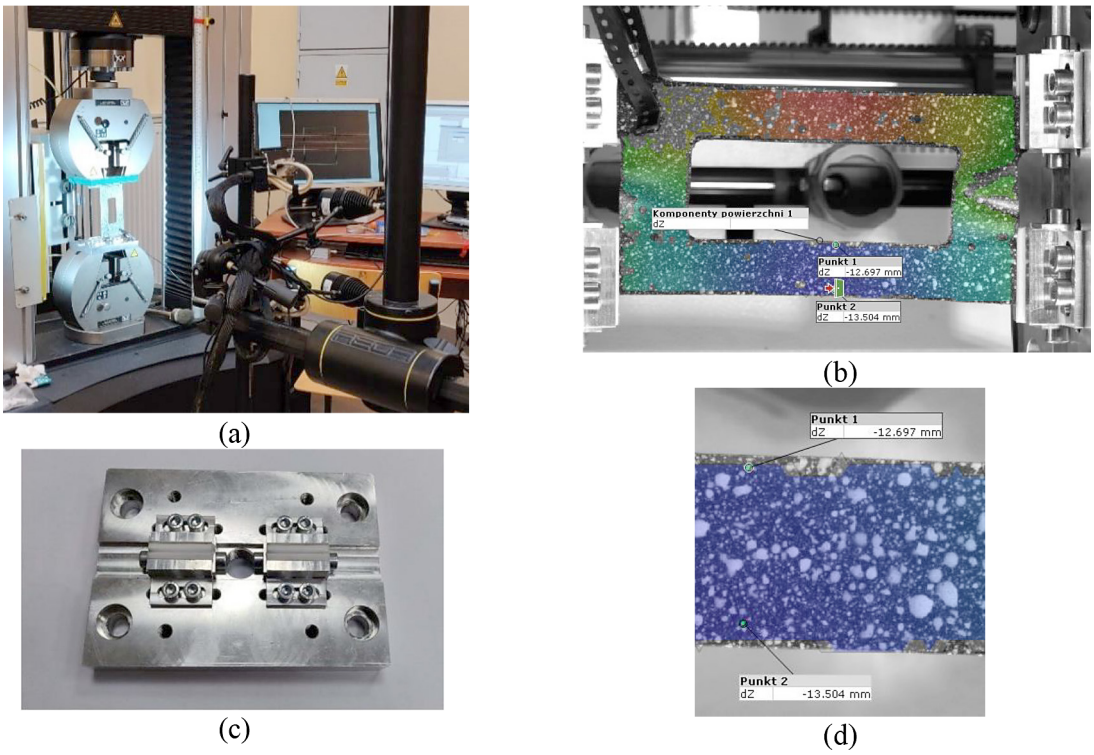

Fig. 2. (a) Experimental test stand, (b) Aramis software view with selected points, (c) specially designed grips, (d) zoom of measured points

4-noded shell elements (S4R) with six degrees of freedom at each node. The numerical model with boundary conditions is presented in Figure 3.

A two-stage solution was considered. The first part of FE modelling was the linear buckling analysis which allows to determine buckling loads with corresponding obtained the lowest bending-torsional buckling modes. The obtained buckling modes have been used as a shape of initial geometrical imperfection. In the second step, the nonlinear analysis using the Newton–Raphson method was peformed. The nonlinear analyses were carried-out with the progressive failure algorithm [31–33]. The results of sample calculations are presented as a shape of buckling form and graphs showing the relation between load and deflection. More details about numerical analysis and the way of discretization presented in articles [20,32].

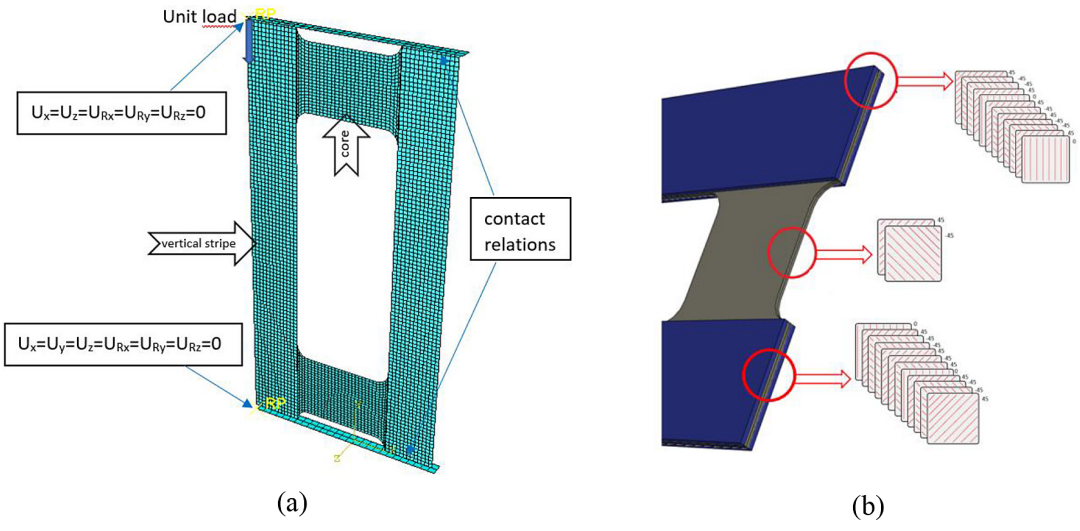

Fig. 3. (a) Discrete model with applied boundary conditions and load, (b) considered laminate plate with exemplary layer arrangement N3(45)

PARAMETRIC STUDY

The parametric study was performed to validate *extension-bending* and *extension-twisting* couplings in plate element. According to the Classical Laminate Theory (CLT), the dependence between internal forces and deformations makes it possible to predict the behavior of the plate under selected loads. The relation between laminate constitutive equation have the following form [8,34–37]:

$$\begin{Bmatrix}\{N\}\\ \{M\}\end{Bmatrix} = \begin{bmatrix}[A] & [B]\\ [B] & [D]\end{bmatrix}\begin{Bmatrix}\{\varepsilon\}\\ \{\kappa\}\end{Bmatrix} \quad (1)$$

where: N and M – internal forces and moments, ε and the mid-plane κ – strains and curvatures of the laminate respectively A, B, D – are the stiffness matrices.

Asymmetric laminates are characterized by the occurrence of additional asymmetric couplings when particular terms of the coupling stiffness matrix are equal to $B_{11} \neq 0$, $B_{12} \neq 0$ and $B_{22} \neq 0$ (normal loads – flexural loads) or $B_{66} \neq 0$ (shearing load – torsional strain) and $B_{16} \neq 0$ and $B_{26} \neq 0$ (normal load – torsional strain). Each of the matrices with the "0" index consists of zeros obviously. The B coupling matrix, besides the B_0 variant, can has additionally five different forms of couplings: B_l, B_t, B_{lt}, B_S and B_F, which were described in detail by York [7,38,39]. Due to mechanical couplings, it is possible to shape the mechanical properties of composite elements by designing the required couplings of strain states. This conception was employed to find solutions for changing the lowest form of buckling from bending to higher flexural-torsional form and thanks to this it made it possible to get elastic element. According to the international literature [8,23,38,39], the used notations for the ABD laminate stiffness matrix are presented in Table 3. The considered in the study cases of layer arrangements are presented in Table 1. Analytical calculations performed for three nonsymmetrical layer configurations the range of layer orientation angle θ from 0 to 90 degrees with a 15-degree step.

Constitutive realtions

The constitutive relations are useful for confirmation occurring couplings, and to gain qualitative insight into the relative twist from additional join terms. Eq. 2-4 present the results of analytical calculations of constitutive relations for the three considered configurations (N1, N2, N3) for an exemplary fiber angle Θ=60°. The calculations were carried out using a Matlab program.

Table 3. Subscript identification method of composite laminate stiffness matrices proposed by the ESDU (1994) [23]

Subscript identification ESDU (1994) [23]	Response – based labelling	Matrix form
A_S	Simple laminate; no coupling	$\begin{bmatrix}A_{11} & A_{12} & 0\\ A_{21} & A_{22} & 0\\ 0 & 0 & A_{66}\end{bmatrix}$
A_F	Shear-Extension coupling; S-E	$\begin{bmatrix}A_{11} & A_{12} & A_{16}\\ A_{21} & A_{22} & A_{26}\\ A_{61} & A_{62} & A_{66}\end{bmatrix}$
B_S	Extension-Bending and Shearing-Twisting coupling; E-B, S-T	$\begin{bmatrix}B_{11} & B_{12} & 0\\ B_{21} & B_{22} & 0\\ 0 & 0 & B_{66}\end{bmatrix}$
B_F	Extension-Bending, Shearing-Bending, Extension-Twisting and Shearing-Twisting; E-B, S-B, E-T, S-T	$\begin{bmatrix}B_{11} & B_{12} & B_{16}\\ B_{21} & B_{22} & B_{26}\\ B_{61} & B_{62} & B_{66}\end{bmatrix}$
B_t	Extension-Twisting and Shearing-Bending coupling; E-T, S-B	$\begin{bmatrix}0 & 0 & B_{16}\\ 0 & 0 & B_{26}\\ B_{61} & B_{62} & 0\end{bmatrix}$
B_l	Extension-Bending coupling; E-B	$\begin{bmatrix}B_{11} & 0 & 0\\ 0 & B_{22} & 0\\ 0 & 0 & 0\end{bmatrix}$
B_{lt}	Extension-Bending, Extension-Twisting and Shearing-Bending coupling; E-B, E-T, S-B	$\begin{bmatrix}B_{11} & 0 & B_{16}\\ 0 & B_{22} & B_{26}\\ B_{61} & B_{62} & 0\end{bmatrix}$
D_S	Simple laminate; no coupling	$\begin{bmatrix}D_{11} & D_{12} & 0\\ D_{21} & D_{22} & 0\\ 0 & 0 & D_{66}\end{bmatrix}$
D_F	Twisting-Bending coupling; T-B	$\begin{bmatrix}D_{11} & D_{12} & D_{16}\\ D_{21} & D_{22} & D_{26}\\ D_{61} & D_{62} & D_{66}\end{bmatrix}$

The ABD matrix for N1(60°) configuration is given in Eq. 2 and represents E-B-E-T-S-B coupling.

$$\begin{Bmatrix} \begin{Bmatrix} N_x \\ N_y \\ N_{xy} \\ \dots \end{Bmatrix} \\ \begin{Bmatrix} M_x \\ M_y \\ M_{xy} \end{Bmatrix} \end{Bmatrix} = \begin{bmatrix} 79847.55 & 29686.80 & 0 & \vdots & -39681.60 & 0 & 174.63 \\ 29686.80 & 152524.47 & 0 & \vdots & 0 & 39681.60 & 486.24 \\ 0 & 0 & 32968.87 & \vdots & 174.63 & 486.24 & 0 \\ \dots & \dots & \dots & \dots & \dots & \dots & \dots \\ & & & \vdots & 34074.13 & 4567.69 & 0 \\ & symmetry & & \vdots & 4567.69 & 43635.87 & 0 \\ & & & \vdots & 0 & 0 & 5544.68 \end{bmatrix} = \begin{Bmatrix} \begin{Bmatrix} \varepsilon_x \\ \varepsilon_y \\ \gamma_{xy} \\ \dots \end{Bmatrix} \\ \begin{Bmatrix} \mathrm{K}_x \\ \mathrm{K}_y \\ \mathrm{K}_{xy} \end{Bmatrix} \end{Bmatrix} \quad (2)$$

The ABD matrix for N2(60°) configuration is given in Eq.3 and represents E-B-S-B-E-T-S-T-T-B coupling.

$$\begin{Bmatrix} \begin{Bmatrix} N_x \\ N_y \\ N_{xy} \\ \dots \end{Bmatrix} \\ \begin{Bmatrix} M_x \\ M_y \\ M_{xy} \end{Bmatrix} \end{Bmatrix} = \begin{bmatrix} 77387.69 & 28801.25 & 0 & \vdots & 5658.12 & -1079.48 & -873.13 \\ 28801.25 & 91923.07 & 0 & \vdots & -1079.48 & -3499.17 & -2431.22 \\ 0 & 0 & 31353.97 & \vdots & -873.13 & -2431.22 & -1079.48 \\ \dots & \dots & \dots & \dots & \dots & \dots & \dots \\ & & & \vdots & 15717.90 & 4846.35 & 73.34 \\ & symmetry & & \vdots & 4846.35 & 15450.81 & 204.22 \\ & & & \vdots & 73.34 & 204.22 & 5306.03 \end{bmatrix} = \begin{Bmatrix} \begin{Bmatrix} \varepsilon_x \\ \varepsilon_y \\ \gamma_{xy} \\ \dots \end{Bmatrix} \\ \begin{Bmatrix} \mathrm{K}_x \\ \mathrm{K}_y \\ \mathrm{K}_{xy} \end{Bmatrix} \end{Bmatrix} \quad (3)$$

The ABD matrix for N3(60°) configuration is given in Eq. 4 and represents E-B-S-B-E-T-S-T-T-B coupling.

$$\begin{Bmatrix} \begin{Bmatrix} N_x \\ N_y \\ N_{xy} \\ \dots \end{Bmatrix} \\ \begin{Bmatrix} M_x \\ M_y \\ M_{xy} \end{Bmatrix} \end{Bmatrix} = \begin{bmatrix} 47086.99 & 28358.47 & 0 & \vdots & 5658.12 & -1079.48 & -174.63 \\ 28358.47 & 90693.14 & 0 & \vdots & -1079.48 & -3499.17 & -486.24 \\ 0 & 0 & 30546.52 & \vdots & -174.63 & -486.24 & -1079.48 \\ \dots & \dots & \dots & \dots & \dots & \dots & \dots \\ & & & \vdots & 7516.83 & 3506.25 & 146.69 \\ & symmetry & & \vdots & 3506.25 & 11202.64 & 408.45 \\ & & & \vdots & 146.69 & 408.45 & 3795.72 \end{bmatrix} = \begin{Bmatrix} \begin{Bmatrix} \varepsilon_x \\ \varepsilon_y \\ \gamma_{xy} \\ \dots \end{Bmatrix} \\ \begin{Bmatrix} \mathrm{K}_x \\ \mathrm{K}_y \\ \mathrm{K}_{xy} \end{Bmatrix} \end{Bmatrix} \quad (4)$$

Laminates N2 and N3 demonstrates that *Bending-Twisting* behaviour is developed because B_{16}, $B_{26} \neq 0$. Hence the addition of *Bending-Twisting* coupling stiffnesses D_{16} and D_{26} in N2 and N3 laminate causes *Twisting* because of *Bending*.

Layer arrangements with their ABD matrix terms

In Figures 4-7 presented the ABD laminate stiffness matrix elements variation, for laminates with different angle of fiber orientation (Θ=0°÷90° with 15° step). The presented curves can be used to estimate which angles θ of the layer arrangements have the extremal value of elements in the coupling stiffness matrix and can have the highest influence on coupled deflection and twist.

Based on the obtained results, can be observed how the values of ABD stiffness matrix elements change with the θ angle. Analyzing the shape of the graphs can be observed that for all considered configurations the graphs shape obtained for [A] element is almost identical for N2 and N3 layer arrangement and for N1 the curves for A11 and A22 components are slightly shifted. A similar situation is for [D] element and in N2 and N3 case for [B] element. However, it should be emphasized here that the number of layers for all selected configurations is different. What is more, very similar shape of graphs in N2 and N3 cases results from the same matrix form and coupling response. It can be noted also, that introducing the additional couplings change the shape of curves. The all components of [B] element are constant for all angles. The change of angle does not influence on level of this element. The graphs shape of components of [B] and [D] laminate stiffness matrices with "16" and "26" (*Bending-Twisting* couplings terms) index for N2 and N3 cases are almost symmetric in relation to each other.

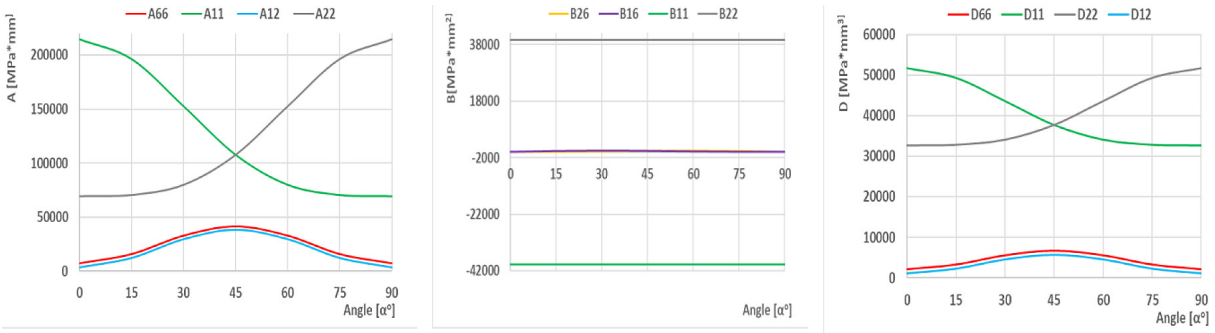

(a) (b) (c)

Fig. 4. Elements (a) [A], (b) [B] and (c) [D] of laminate stiffness matrix value for case N1(θ)

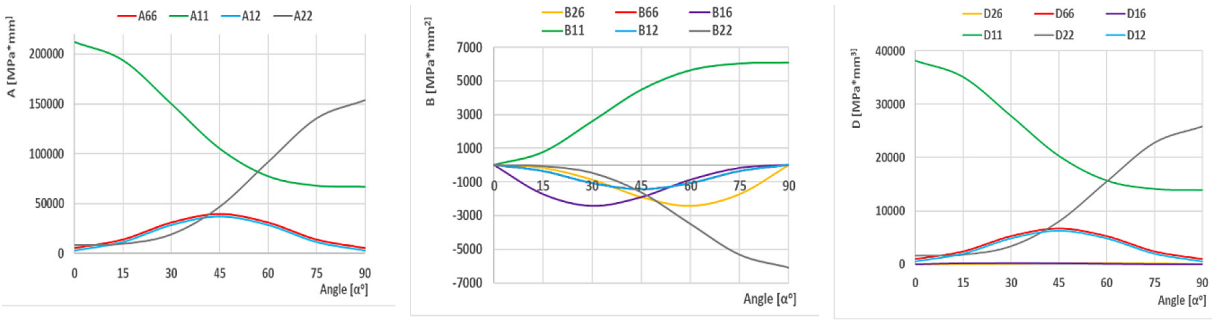

(a) (b) (c)

Fig. 5. Elements (a) [A], (b) [B] and (c) [D] of laminate stiffness matrix value for case N2(θ)

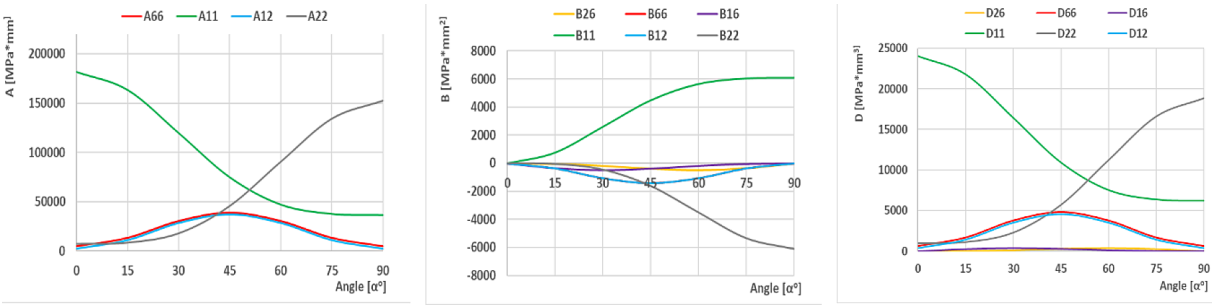

(a) (b) (c)

Fig. 6. Elements (a) [A], (b) [B] and (c) [D] of laminate stiffness matrix value for case N3(θ)

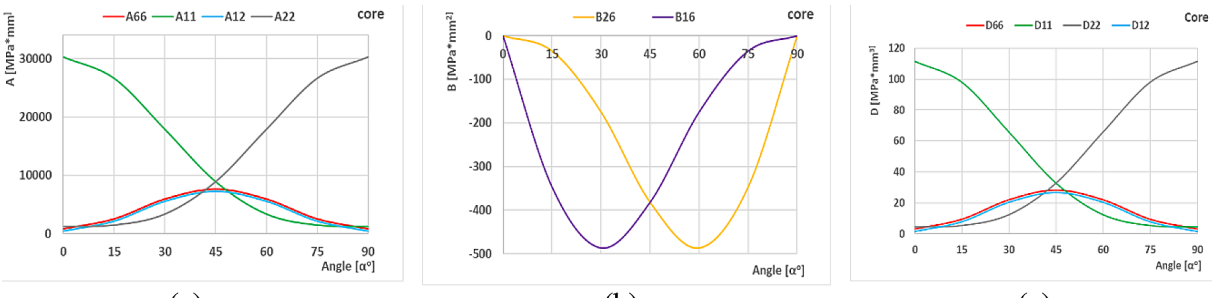

(a) (b) (c)

Fig. 7. Elements (a) [A], (b) [B] and (c) [D] of laminate stiffness matrix value for case N4(θ) - core

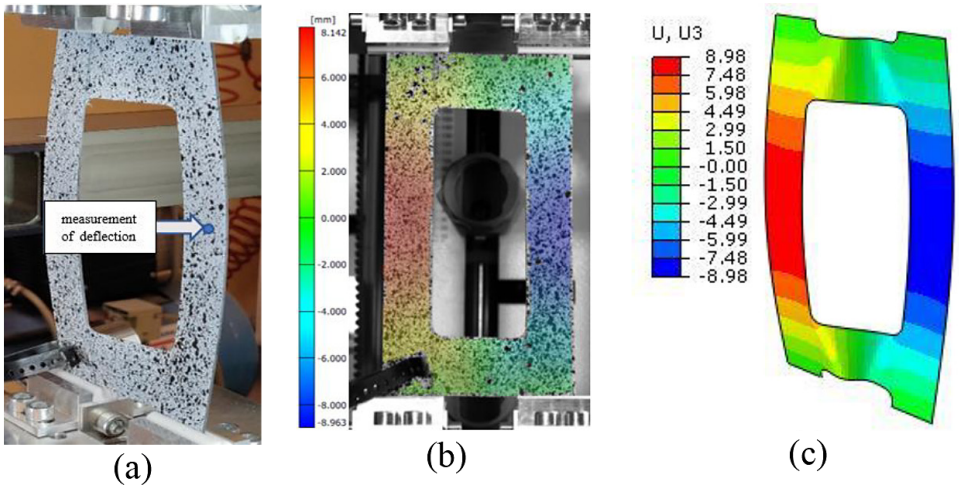

Fig. 8. Comparison of plate deflection for N3(45°) obtained (b) experimentally, (c) numerically

VALIDATION OF NUMERICAL MODEL BY EXPERIMENTAL TESTS

The numerical model has been validate by results of experimental tests. Exemplary results for plate with N3(45°) layer arrangement obtained experimentally and numerically are presented in Figure 8 and 9. For all considered samples the displacement, deflection results from FEM analysis and experimental tests were very similar. This also applied the buckling mode.

Additionally, in Figure 10 presented the exemplary post-critical equilibrium paths P – t (load – time) compared with acoustic emission signal for N1(45) configuration, obtained experimentally. What is more, in damage initiation point and failure point presented shape of plate showing the deflection level of strips.

Layers arrangement influence on load-deflection curves

In Figures 11-13 presented the relations between compression force and twist/rotation value

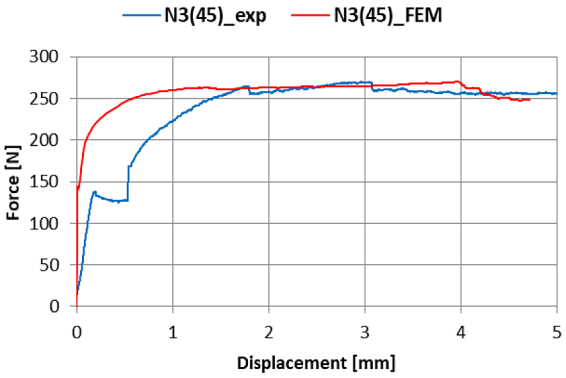

Fig. 9. Compression load vs. displacement for N3(45) sample obtained numerically and experimentally

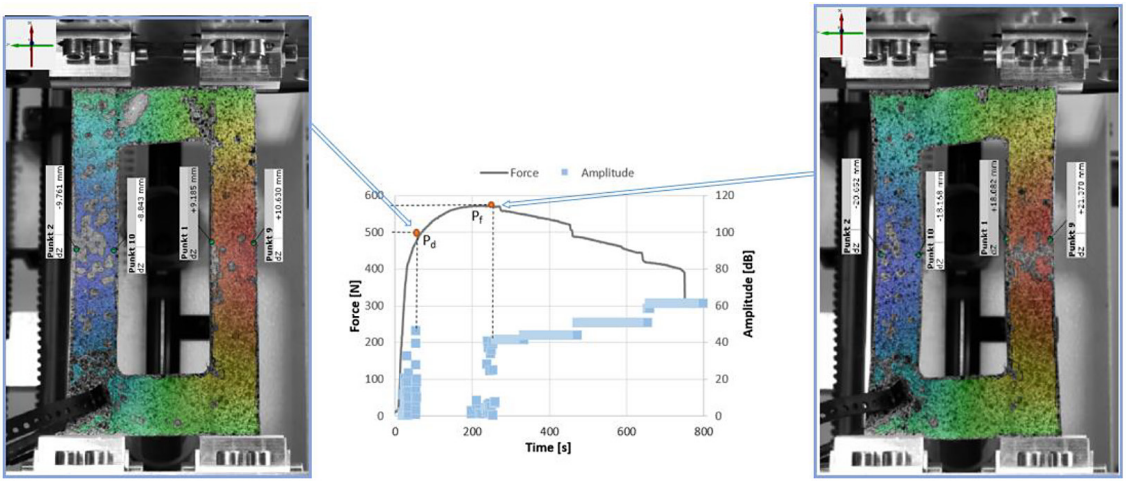

Fig. 10. Post-critical equilibrium paths P – t (load – time) compared with acoustic emission signal – specimen $N1(45)_{exp}$ together with shape of plate located in damage initiation point and failure point

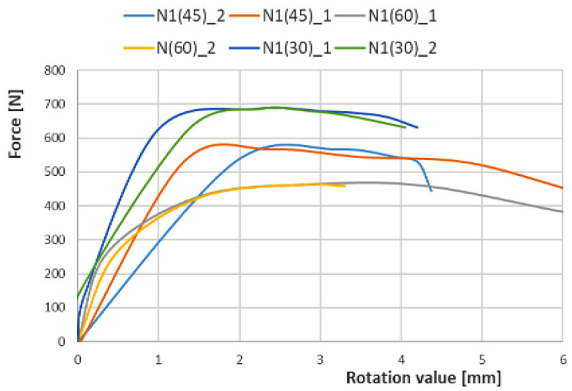

Fig. 11. Compression load vs. rotation value for plate with layups denoted as N1(θ) E-B-E-T-S-B

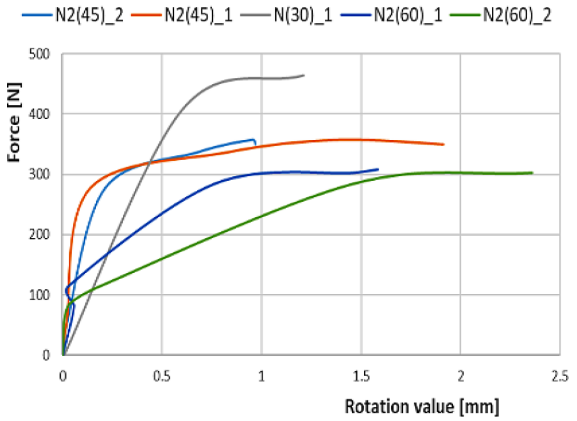

Fig. 12. Compression load vs. rotation value for plate with layups denoted as N2(θ) E-B-S-B-E-T-S-T-T-B

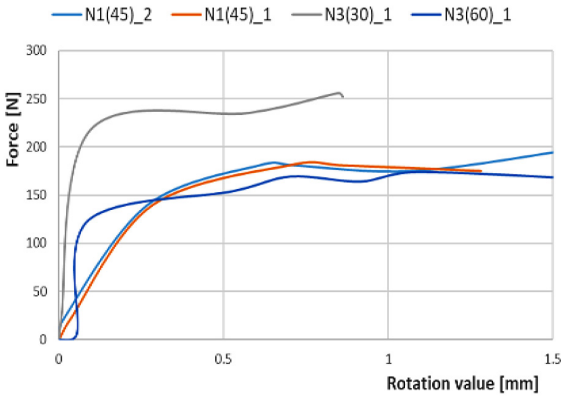

Fig. 13. Compression load vs. rotation value for plate with layups denoted as N3(θ) E-B-S-B-E-T-S-T-T-B

for all tested configurations. For some samples, measurements were made for two strips of the plate - on one side and on the other side. Unfortunately, points were not captured for all samples. This was due to less precise preparation of samples for the Aramis system as well as system settings and available light.

Analyzing all cases it could be noted that the highest stiffness with the lowest rotation value was obtained for layer arrangement with angle of 60°, what is confirmed on graphs presented the ABD laminate stiffness matrix elements variation (Fig. 4-7). It can be observed that type of layer arrangement and type of couplings influence on postcritical behavior tested elements as well on rotation value. In all considered cases, the rotation value is increasing significantly when load is around the buckling load. What is more it can be observed that introduce the laminate coupling responses lead to an increase in twisting response of the specimen. Based on obtained results there is clear evidence that coupling interactions take place, and that these serve to augment the twisting response.

CONCLUSIONS

This study has presented an experimental and analytical validation for asymmetric laminate designs with matched couplings like: *Extension-Twisting* and *Extension-Bending* coupling, which were used to design elastic element. The research study has been focused on the ply sequences expected to have the strongest effect on getting the flexural-torsional buckling mode as the natural the lowest mode of buckling of plate element.

Based on the obtained results, it can be concluded that there is clear evidence that coupling interactions occur in asymmetric layer arrangements, which serve to enhance torsion and bending reactions. When extension-bending and extension-twisting coupled laminates is used to construct bending-twisting coupled structures, the extension-bending and extension-twist coupled effect will cause bending and torsional deformation of opposite direction for one and the other strip of plate. Indeed, the experimentally and analytically validated simulations have confirmed the performance *Extension-Twisting* and *Extension-Bending* coupling.

The performed analysis indicate an area of research that is worth further analysis - how by appropriate selection of matrix components we can influence on the structures behavior.

Acknowledgements

This research was carried out under the National Science Centre of Poland under project No. UMO-2022/47/B/ST8/00600.

Funding

The grant was financed in the framework of the pro-quality program of Lublin University of Technology "Grants for grants" (6/GnG/2023).

REFERENCES

1. Falkowicz K, Debski H, Teter A. Design solutions for improving the lowest buckling loads of a thin laminate plate with notch, Lublin, Poland: 2018, p. 080004. https://doi.org/10.1063/1.5019075.
2. Rozylo P, Falkowicz K, Wysmulski P, Debski H, Pasnik J, Kral J. Experimental-Numerical Failure Analysis of Thin-Walled Composite Columns Using Advanced Damage Models. Materials 2021;14:1506. https://doi.org/10.3390/ma14061506.
3. Kubiak T, Urbaniak M, Kazmierczyk F. The Influence of the Layer Arrangement on the Distortional Post-Buckling Behavior of Open Section Beams. Materials 2020;13:3002. https://doi.org/10.3390/ma13133002.
4. Banat D, Mania RJ. Progressive failure analysis of thin-walled Fibre Metal Laminate columns subjected to axial compression. Thin-Walled Structures 2018;122:52–63. https://doi.org/10.1016/j.tws.2017.09.034.
5. Wysmulski P, Debski H, Falkowicz K. Sensitivity of Compressed Composite Channel Columns to Eccentric Loading. Materials 2022;15:6938. https://doi.org/10.3390/ma15196938.
6. Wysmulski P, Teter A, Debski H. Effect of load eccentricity on the buckling of thin-walled laminated C-columns, Lublin, Poland: 2018, p. 080008. https://doi.org/10.1063/1.5019079.
7. York CB. Unified Approach to the Characterization of Coupled Composite Laminates: Benchmark Configurations and Special Cases. J Aerosp Eng 2010;23:219–42. https://doi.org/10.1061/(ASCE)AS.1943-5525.0000036.
8. York CB. On tapered warp-free laminates with single-ply terminations. Composites Part A: Applied Science and Manufacturing 2015;72:127–38. https://doi.org/10.1016/j.compositesa.2015.01.022.
9. York CB, Lee KK. Test validation of extension-twisting coupled laminates with matched orthotropic stiffness. Composite Structures 2020;242:112142. https://doi.org/10.1016/j.compstruct.2020.112142.
10. Cross RJ, Haynes RA, Armanios EA. Families of Hygrothermally Stable Asymmetric Laminated Composites. Journal of Composite Materials 2008;42:697–716. https://doi.org/10.1177/0021998308088597.
11. Teter A, Mania RJ, Kolakowski Z. Effect of selected elements of the coupling stiffness submatrix on the load-carrying capacity of hybrid columns under compression. Composite Structures 2017;180:140–7. https://doi.org/10.1016/j.compstruct.2017.08.001.
12. Chia C-Y. Nonlinear analysis of plates. New York ; London: McGraw-Hill International Book Co; 1980.
13. Falkowicz K, Samborski S, Valvo PS. Effects of Elastic Couplings in a Compressed Plate Element with Cut-Out. Materials 2022;15:7752. https://doi.org/10.3390/ma15217752.
14. Altenbach H., Altenbach J.W., Kissing W. Mechanics of composite structural elements. Berlin Heilderberg: Springer; 2013.
15. Rzeczkowski J, Samborski S, Valvo PS. Effect of stiffness matrices terms on delamination front shape in laminates with elastic couplings. Composite Structures 2020;233:111547. https://doi.org/10.1016/j.compstruct.2019.111547.
16. Samborski S. Analysis of the end-notched flexure test configuration applicability for mechanically coupled fiber reinforced composite laminates. Composite Structures 2017;163:342–9. https://doi.org/10.1016/j.compstruct.2016.12.051.
17. York CB. On Extension–Shearing coupled laminates. Composite Structures 2015;120:472–82. https://doi.org/10.1016/j.compstruct.2014.10.019.
18. York CB, de Almeida SFM. On Extension-Shearing Bending-Twisting coupled laminates. Composite Structures 2017;164:10–22. https://doi.org/10.1016/j.compstruct.2016.12.041.
19. York CB, de Almeida SFM. Effect of bending-twisting coupling on the compression and shear buckling strength of infinitely long plates. Composite Structures 2018;184:18–29. https://doi.org/10.1016/j.compstruct.2017.09.085.
20. Falkowicz K, Debski H. Stability analysis of thin-walled composite plate in unsymmetrical configuration subjected to axial load. Thin-Walled Structures 2021;158:107203. https://doi.org/10.1016/j.tws.2020.107203.
21. Falkowicz K, Debski H, Wysmulski P. Effect of extension-twisting and extension-bending coupling on a compressed plate with a cut-out. Composite Structures 2020;238:111941. https://doi.org/10.1016/j.compstruct.2020.111941.
22. Falkowicz K, Szklarek K. Analytical method for projecting the buckling form of composite palates with a cut-out. IOP Conf Ser: Mater Sci Eng 2019;710:012021. https://doi.

org/10.1088/1757-899X/710/1/012021.

23. ESDU. Stiffnesses of laminated plates. Engineering sciences data unit, Item no. 94003 1994.
24. Różyło P, Smagowski W, Paśnik J. Experimental Research in the Aspect of Determining the Mechanical and Strength Properties of the Composite Material Made of Carbon-Epoxy Composite. Adv Sci Technol Res J 2023;17:232–46. https://doi.org/10.12913/22998624/161598.
25. Falkowicz K, Dębski H, Wysmulski P, Różyło P. The behaviour of compressed plate with a central cut-out, made of composite in an asymmetrical arrangement of layers. Composite Structures 2019;214:406–13. https://doi.org/10.1016/j.compstruct.2019.02.001.
26. Jonak J, Karpiński R, Siegmund M, Wójcik A, Jonak K. Analysis of the Rock Failure Cone Size Relative to the Group Effect from a Triangular Anchorage System. Materials 2020;13:4657. https://doi.org/10.3390/ma13204657.
27. Machrowska A, Karpiński R, Jonak J, Szabelski J, Krakowski P. Numerical prediction of the component-ratio-dependent compressive strength of bone cement. Applied Computer Science 2020:88–101. https://doi.org/10.23743/acs-2020-24.
28. Jonak J, Karpiński R, Wójcik A. Numerical analysis of the effect of embedment depth on the geometry of the cone failure. J Phys: Conf Ser 2021;2130:012012. https://doi.org/10.1088/1742-6596/2130/1/012012.
29. Jonak J, Karpiński R, Wójcik A, Siegmund M. Numerical Investigation of the Formation of a Failure Cone during the Pullout of an Undercutting Anchor. Materials 2023;16:2010. https://doi.org/10.3390/ma16052010.
30. Falkowicz K. Stability Analysis of Thin-Walled Perforated Composite Columns Using Finite Element Method. Materials 2022;15:8919. https://doi.org/10.3390/ma15248919.
31. Falkowicz K. Experimental and numerical failure analysis of thin-walled composite plates using progressive failure analysis. Composite Structures 2023;305:116474. https://doi.org/10.1016/j.compstruct.2022.116474.
32. [32] Falkowicz K, Ferdynus M, Rozylo P. Experimental and numerical analysis of stability and failure of compressed composite plates. Composite Structures 2021;263:113657. https://doi.org/10.1016/j.compstruct.2021.113657.
33. Rozylo P, Falkowicz K. Stability and failure analysis of compressed thin-walled composite structures with central cut-out, using three advanced independent damage models. Composite Structures 2021;273:114298. https://doi.org/10.1016/j.compstruct.2021.114298.
34. Carl T. Herakovich H. Mechanics of fibrous composites. New York: Wiley and Sons; 1998.
35. Haynes R, Cline J, Shonkwiler B, Armanios E. On plane stress and plane strain in classical lamination theory. Composites Science and Technology 2016;127:20–7. https://doi.org/10.1016/j.compscitech.2016.02.010.
36. Jones RM. Mechanics of Composite Materials. 2nd ed. CRC Press; 2018. https://doi.org/10.1201/9781498711067.
37. Samborski S. Numerical analysis of the DCB test configuration applicability to mechanically coupled Fiber Reinforced Laminated Composite beams. Composite Structures 2016;152:477–87. https://doi.org/10.1016/j.compstruct.2016.05.060.
38. York C. Unified approach to the characterization of coupled composite laminates: Hygro-thermally curvature-stable configurations. International Journal of Structural Integrity 2011;2:406–36. https://doi.org/10.1108/17579861111183920.
39. York CB. Tapered hygro-thermally curvature-stable laminates with non-standard ply orientations. Composites Part A: Applied Science and Manufacturing 2013;44:140–8. https://doi.org/10.1016/j.compositesa.2012.08.023.